Identification of candidate protein markers of Bovine Parainfluenza Virus Type 3 infection using an in vitro model

Gray, D. W., Welsh, M. D., Doherty, S., & Mooney, M. H. (2017). Identification of candidate protein markers of Bovine Parainfluenza Virus Type 3 infection using an in vitro model. Veterinary Microbiology. DOI: 10.1016/j.vetmic.2017.03.013

Published in:
Veterinary Microbiology

Document Version:
Peer reviewed version

Queen's University Belfast - Research Portal:
Link to publication record in Queen's University Belfast Research Portal

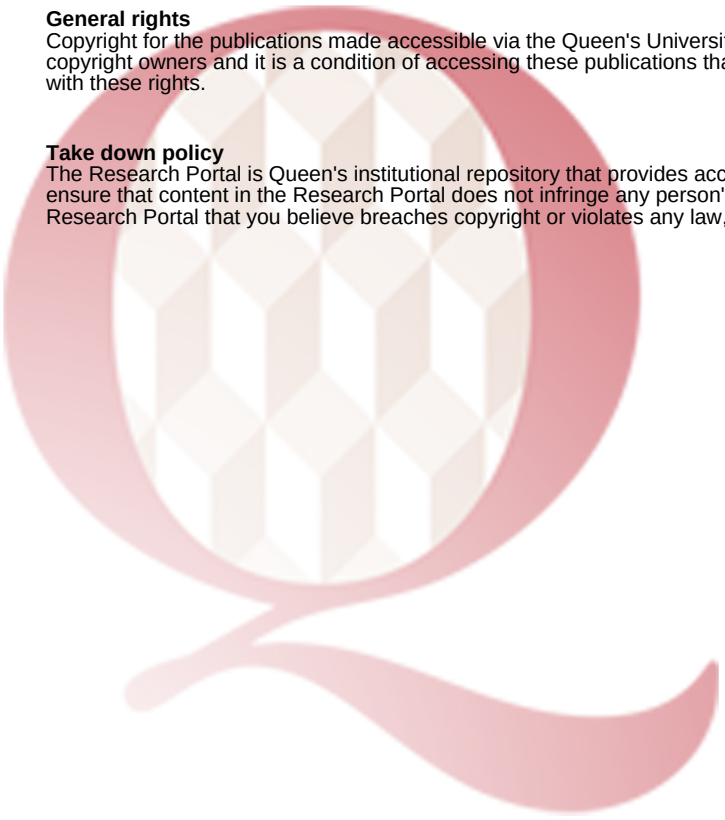

Identification of candidate protein markers of Bovine Parainfluenza Virus Type 3 infection using an *in vitro* model

Darren W Gray*[†], Michael D Welsh[#], Simon Doherty[#], and Mark H Mooney[†]

[†]Institute for Global Food Security (IGFS), School of Biological Sciences, Queen's University Belfast (QUB), Belfast, Northern Ireland, BT9 5AG, United Kingdom

[#]Veterinary Sciences Division (VSD), Agri-Food and Biosciences Institute (AFBI), Belfast, Northern Ireland BT4 3SD, United Kingdom

*Corresponding author's address:

Institute for Global Food Security,

School of Biological Sciences,

Queen's University Belfast,

David Keir Building,

Stranmillis Road,

Belfast,

BT9 5AG,

United Kingdom

Phone: +44(0)28 90976542

Fax: +44 (0)28 90976513

Email: d.gray@qub.ac.uk

Abstract

Bovine Parainfluenza Virus Type 3 (BPI3V) infections are often asymptomatic, causing respiratory tissue damage and immunosuppression, predisposing animals to severe bacterial pneumonia, the leading cause of Bovine Respiratory Disease (BRD) mortality. As with many pathogens, routine BPI3V serology does not indicate the presence of damaged respiratory tissue or active infection. *In vitro* proteomic marker screening using disease relevant cell models could help identify markers of infection and tissue damage that are also detectable during *in vivo* infections. This study utilised a proteomic approach to investigate *in vitro* cellular responses during BPI3V infection to enhancing the current understanding of intracellular host-virus interactions and identify putative markers of *in vivo* infection. Through 2D gel electrophoresis proteomic analysis, BPI3V Phosphoprotein P and host T-complex Protein 1 subunit theta were found to be accumulated at the latter stages of infection within bovine fibroblasts. These proteins were subsequently detected using targeted multiple reaction monitoring (MRM) mass spectrometry in the plasma of animals challenged with BPI3V, with differential protein levels profile observed dependant on animal vaccination status. Potential mechanisms by which BPI3V overcomes host cellular immune response mechanisms allowing for replication and production of viral proteins were also revealed. Assessment of circulating protein marker levels identified through an *in vitro* approach as described may enable more effective diagnosis of active viral infection and diseased / damaged respiratory tissue in animals and allow for more effective utilisation of preventative therapeutic interventions prior to bacterial disease onset and significantly aid the management and control of BRD.

Introduction

Bovine Respiratory Disease (BRD) is a multifactorial disease characteristic of a viral-bacterial synergistic infection with predisposition from environmental stressors. The disease constitutes a major source of economic loss through mortality, clinical disease and associated treatments with long lasting reduced growth performance of infected young stock (Griffin, 1997). Bovine Parainfluenza Virus-3 (BPI3V) is one of the major viral pathogens of the BRD complex (Kahrs, 2001). BPI3V induced respiratory tract damage, resulting from the destruction of the ciliated respiratory epithelium (Bryson, 1985) and immunosuppression via depression of local cellular immunity by impairment of alveolar macrophage phagocytosis (Baker et al., 1997, Trigo et al., 1985), predisposes animals to more severe secondary bacterial and mycoplasma infections (Cusack et al., 2003, Kapil and Basaraba, 1997). With the absence of severe clinical symptoms (Vaucher et al., 2008), infected animals may not be detected prior to the onset of more severe infections (AFBI/DAFM, 2012). Furthermore, routinely employed BPI3V-antibody ELISA cannot differentiate between vaccinated and infected animals, and by the time infected animals convalesce the virus has been cleared from the system and respiratory tract damage has already occurred. Molecular diagnostic techniques are hindered by the presence of vaccine derived genetic material, often requiring on-going virus amplification in order to generate sufficient genetic material for accurate diagnosis. Consequently, there are no commercial tests available for differentiation between BPI3V vaccinated and non-vaccinated animals. Anti-mortem diagnostic tests for BPI3V such as immunohistochemistry and virus isolation provide limited information on the current health status of an animal and can only determine pathogen exposure but not the presence of diseased tissue (Fulton and Confer, 2012), further illustrating the need for the development of alternative diagnostics capable of detecting infected animals (and the presence of diseased tissue) at early stages of infection.

The development of biomarker based diagnostic tests relies on the detection of disease markers accumulated/released from localised tissues regions in circulating bio-fluids. Primary cell

cultures offer a clean system that closely resembles relative tissue types for the identification of high confidence candidate markers for *in vivo* diagnostics. With the death of BPI3V infected cells, proteins are released into the extracellular space and ultimately into circulating bio-fluids. The detection of such markers would indicate not only the presence of viral infection but also damaged respiratory tissue, an indicator of underlying disease. Suitable primary cell models to investigate BPI3V associated tissue damage include epithelial cells (the initial site of infection) and fibroblasts (the major component of lung interstitium and likely secondary site of infection following BPI3V release from epithelial cells). Whilst epithelial cells are the most promising cell types for candidate biomarker screening previous studies on Human Parainfluenza Virus-3 (hPIV-3) and the closely related paramyxovirus Respiratory Syncytial Virus (RSV) in A549 adenocarcinomic human alveolar basal epithelial cells have indicated an apoptotic response to infection, with an arrest in protein production (van Diepen et al., 2010, Brasier et al., 2004). Such condidtions are unfavourable for biomarker screening which relies on the accumulation of disease specific markers within tissues and their eventual release into circulating biofluids. Foetal Calf Lung (FCL) cells are known to facilitate *in vitro* growth of BPI3V (Shephard et al., 2003) and may provide conditions favourable for viral replication without shut down of host protein production, however little is understood about the interactions of BPI3V with respiratory fibroblasts at the intracellular level. Therefore, this study has set out to assess the proteomic responses of FCL cells during an *in vitro* BPI3V infection by 2 Dimensional Gel Electrophoresis (2D GE) profiling, and to determine whether identified candidate protein markers of *in vitro* infection can also be observed within the plasma of animals following *in vivo* infection. Such markers released from infected cells or diseased tissue, could be utilised to not only diagnose animals exposed to the viral pathogens but also determine virus induced respiratory tract damage and enable early treatment measures to be employed to prevent progression to more severe clinical disease states.

Materials and methods

Chemicals and reagents

GMEM, trypsin, gentamicin and glutamine were purchased from Invitrogen (Life Technologies, Paisley, UK). Dithiothreitol (DTT), iodoacetamide (IAA), and Readysol IEF were purchased from GE Healthcare (Buckinghamshire, UK). LC-MS grade formic acid, acetonitrile and H_2O were purchased from Fisher Scientific (MA, USA). All other reagents were electrophoresis grade and purchased from Fisher Scientific. Sequencing grade modified trypsin was purchased from Promega (WI, USA).

In vitro identification of candidate BPI3V protein biomarkers

Cell culture and virus preparation

Foetal Calf Lung (FCL) cells were prepared within the cell culture department of the Veterinary Science Division at the Agri-Food and Biosciences Institute, Northern Ireland. Throughout this study FCL cells were maintained at 37ºC, 5% CO_2 and adapted to low serum conditions via continuous passage in GMEM (supplemented with 1% glutamine, 0.1% gentamicin) with reducing foetal calf serum (FCS) concentration. Following adaption, cell viability and integrity was assessed by Alamar Blue (Invitrogen) and lactose dehydrogenase (LDH) (Roche, Basel, Switzerland) cytotoxicity assays using manufacturer's protocols.

Preparation of samples for *in vitro* biomarker screening

FCL cells were seeded at a density of $6.25x10^5$ cells per ml in 375ml culture flasks. Cells were grown for 4 days until monolayered, then infected with BPI3V (isolate 2005/015033-Lung A – propagated in FCL cells ($TCID_{50}$ $10^{8.2}$/ml)) a m.o.i. of 10:1 and incubated for 1hr. Media was removed and cells washed 3 times with GMEM containing no FCS which was removed and replaced with GMEM containing 0.5% FCS. Lysates were prepared from BPI3V infected FCL flasks at 24hrs and 48hrs (n=6) post-infection (p.i.). 27hrs prior to sample collection, media was

removed and cells washed 3 times over a period of 3hrs with GMEM containing no FCS. Then washing media was removed and replaced with GMEM continuing no supplements. After 24hrs culture media was removed from flasks and FCL monolayers washed twice with PBS and 1ml of Lysis buffer (7M Urea, 2M Thiourea, 4% CHAPS, Roche Protease Inhibitor (1 tablets per 10ml buffer) (Roche Applied Science, Lewes, East Sussex, United Kingdom) added and incubated for 15min to facilitate cell lysis prior to protein concentration determination. Lysates were similarly prepared from uninfected cells (0hrs, n=6) as control.

2D Gel Electrophoresis and image acquisition

Cellular lysates were concentrated and desalted using 10kDa MW cut-off devices (Millipore, MA, USA) and 500µg of each sample was dissolved in rehydration buffer (final concentration 8M Urea, 2% CHAPS, 0.5% IPG buffer, 0.002% bromophenol blue and 18mM DTT) and allowed to rehydrate overnight with IEF strips. 2D GE was performed using 13cm pH 3-10 non-linear IPG strips (GE Healthcare, Buckinghamshire, UK) in the first dimension and 12.5% SDS PAGE in the second dimension as described previously (Kinkead et al., 2015). Gels were fixed and stained using the LSB colloidal staining method (Anderson et al., 1995), scanned using an Epson Perfection v750 Pro scanner calibrated with a Monaco iT8 transparency reference target (iT8.7/1-1993 MONT45:2010:12) and analysed using Ludesi REDFIN v3 software (Kafoo Group, Sweden). Gel images from analysis of pooled samples were used as a reference for warping and spot matching - approximately 20 manual warping anchors were applied to all gels prior to automatic alignment. Spot borders and locations were manually refined to ensure accurate location and matching prior to spot selection.

Mass-spectrometry analysis of protein gel spots

Gel spots were excised using a Gelpal spot cutter (Genetix) from pooled FCL lysates (comprised of an equal amount of all samples, n=3) and in gel digestion was performed using modifications to a

previously described protocol (Shevchenko et al., 2006). Digests were evaporated to dryness using a MiVac Quattro Concentrator operating under aqueous settings for 4hr at 30ºC. Tryptic peptides were resuspended in 12µl of a 0.1% formic acid, 2% acetonitrile solution and analysed using a Thermo Scientific LTQ ORBITRAP XL mass spectrometer connected to a Dionex Ultimate 3000 (RSLCnano) chromatography system. Each sample was loaded onto a Biobasic Picotip Emitter (120mm length, 75µm ID) packed with Reprocil Pur C18 (1.9µm) reverse phase media column and separated by an increasing acetonitrile gradient, using a 19min reverse phase gradient at a flow rate of 250nL/min. The mass spectrometer was operated in positive ion mode with a capillary temperature of 200°C, a capillary voltage of 31V, a tube lens voltage of 85V and with a potential of 1900V applied to the frit. All data was acquired with the mass spectrometer operating in automatic data dependent switching mode. A high-resolution MS scan (mass range of 300-2000Da) was performed using the Orbitrap to select the 7 most intense ions prior to MS/MS analysis using the Ion trap.

Protein identification and functional classification

Raw mass spectrometry data was processed and de novo peptide analysis performed using PEAKS Studio version 6 (Bioinformatics Software Inc.). Parent mass tolerance and fragment ion error were set at 20ppm and 1.0Da respectively. A maximum of 3 missed cleavages and 1 non-specific cleavage were allowed. A fixed Post Translational Modifications (PTM) of carbamidomethylation was selected and a maximum of 3 variable PTMs per peptide. Peptides were searched against a combined Uniprot *Bos Taurus* and Bovine Parainfluenza Virus-3 database. A false discovery rate of 1% was applied with the requirement of at least 1 unique peptide per protein match. Correct identification was only allowed for peptides that corresponded to a protein with matching molecular weight and pI on 2D gels. The Panther database (version 8.1, http://www.pantherdb.org/) was used for functional classification of identified proteins. As the bovine proteome lacks high-level annotation as compared to the human proteome, missing functional classifications were determined

based on human homologues. Where functional classification could not be determined using Panther, AmiGO (version 1.8, http://amigo.geneontology.org/cgi-bin/amigo/go.cgi) experimental evidence code gene ontology annotations were selected.

In vivo assessment of candidate BPI3V protein biomarkers

BPI3V infection protein marker candidates selected from *in vitro* proteomic analysis were screened in bio-banked plasma samples from BPI3V challenged vaccinated and non-vaccinated calves (Gray et al., 2015).

In-solution tryptic digestion of proteins for targeted MRM analysis by UPLC-MS/MS

10µl of 1µM yeast ADH (internal recovery control) and 20µl of plasma was diluted to a final volume of 100µl with 100mM ammonium bicarbonate. Samples were reduced with 10µl of 100mM DTT, 100mM ammonium bicarbonate for 60ºC for 30mins followed by alkylation with 10µl of 200mM iodoacetamide, 100mM ammonium bicarbonate for 1hr. 50µl of Promega sequencing grade trypsin (80µg/ml in 10% acetonitrile, 10mM ammonium bicarbonate) was added and samples were incubated at 37ºC for 16hrs. 10µl of 10% formic acid was then added to stop the reaction and peptides were purified and concentrated by C18 solid phase extraction (SPE) using an Empore C18 96 well solid phase extraction (SPE) plate (Sigma Aldrich). The resin was conditioned with 100µl of 0.1% formic acid, 99.9% acetonitrile and washed twice with 200µl 0.1% formic acid (wash buffer) prior to addition of digested samples. The plate was washed with 200µl of wash buffer and peptides eluted with three washes of 150µl 0.1% formic acid, 60% acetonitrile. The combined eluates were dried using a MiVac (GeneVac) operating at 40ºC H_2O.

Targeted MRM analysis of peptides by UPLC-MS/MS

In silico peptide fragmentation and selection of MRM transitions (Supplementary File 1) was performed using Skyline (MacLean et al., 2010) and BLAST search performed by MRMpath

(Crasto et al., 2013). Dried peptides were reconstituted in 20µl 0.1% formic acid, 3% acetonitrile, 96.9% H_2O and 8µl of sample was injected onto an ACQUITY UPLC® CSHT130 C18 column (100mm x 2.1mm i.d., 1.7µm, 130Å; Waters Corporation, Milford, MA, USA). Column and autosampler temperature were maintained at 30ºC and 8ºC respectively, and chromatographic separation performed at a flow rate of 100µl/min with mobile phase consisting of 99.9% H_2O, 0.1% formic acid (A) and 99.9% Acetonitrile, 0.1% formic acid (B). The elution gradient was as follows: 0 – 1 min isocratic at 1% of B, 1 – 30 min linear gradient from 1 - 45% of B, 30 – 31 linear gradient from 45 - 95% of B, 31 – 33 min isocratic at 95% of B, 33 min at isocratic 1% B and finally 33 – 35 min isocratic at 1% of B. Mass spectrometry was performed using a Waters Quattro Premier QqQ operating in positive-ion mode (ESI+) with the capillary voltage set to 3000V and the sampling cone voltage 35V. The desolvation, collision and cone gas flows were set at 500 L/h, 0.3 ml/min and 50 L/h respectively. Source and desolvation temperatures were 120ºC and 400ºC respectively. Inter-channel and inter-scan delay were maintained at 0.005s, scan range at 0.5Da, and dwell at 0.025s for all peptides.

Statistical analysis

Two-way ANOVA with post-hoc bonferroni test was applied for the analysis of FCS media content and BPI3V infection in Alamar Blue cell viability and LDH cell cytotoxicity assays. Significantly different protein spots were selected using ANOVA within Ludesi Redfin software. Linear and non-linear regression for protein quantification and correlation between estimated and identified protein MW and pI was performed using Prism Graphpad version 5. SIMCA version 13 (Umetrics) was employed for multivariate statistical analysis of spot volumes obtained from 2D GE. Principle component analysis was applied to Pareto scaled data, excluding spots with %CV greater than 50%. For targeted peptide analysis by UPLC-MS, ANOVA with bonferroni post-hoc test was performed for statistical analysis using Prism Graphpad (version 5). Statistical analysis of temporal changes in protein levels between experimental groups throughout the study was assessed using a paired two-

tailed t-test. TargetLynx was used for the extraction of raw data and analysis. Integration parameters were: retention time window 0.2 min, mean smoothing, width 3, 3 iterations, automatic apex peak tracking and integration window extend of 5. Peak area values for the respective peptides were corrected using the peak area of internal trypsin self-digestion products and spiked yeast ADH was employed to assess peptide recovery. ADH standards in the range of 100µM to 10nM facilitated the relative quantification of protein levels in plasma.

Results

In vitro identification of candidate BPI3V markers of infection

Optimization of *in vitro* models for BPI3V infection studies

Adaption of FCL cells to low serum growth conditions (to minimize contamination of cell lysates with serum derived proteins) had no negative impact on viability or integrity of cells throughout the sample collection period (Supplementary File 2). Increased cytotoxicity and decreased cell viability were observed as a result of BPI3V infection at 72hrs p.i. thereby restricting the sampling period to 48hrs p.i.

Identification of *in vitro* BPI3V infection markers by 2D GE analysis of FCL lysates

Figure 1 illustrates representative gel images obtained following 2D GE analysis of mock/BPI3V infected FCL lysates. 2D gels revealed excellent protein separation and resolution by pI and MW, with an average of 738 spots detected within FCL lysates across all gels. Spots identified visually as being significantly different within infected compared to control FCL cells are indicated. 57 spots were found to have fold change (FC) >1.5 (up- or down-regulated relative to 0hrs mock infected FCL cells) and $p<0.05$ from one-way ANOVA (performed in Ludesi software) (Supplementary File 3), representing an alteration of 19% of detectable proteins in response to BPI3V infection. These spots (illustrated in Figure 1) were selected for protein identification by liquid chromatography mass spectrometry (LC-MS).

253

254 **LC-MS identification of differentially expressed protein spots**

255 The identity and sequence coverage of the 57 spots analysed by LC-MS are illustrated in Table 1.
256 The estimated MW and pI of selected spots were determined by matching against a reference gel
257 map for MRC-5 fibroblasts (Rubporn et al., 2009). Data analysis was performed using Peaks
258 Studio (version 6) and 53 of 57 spots submitted for LC-MS were identified against a combined
259 Uniprot KB *Bos taurus* and BPI3V database. Blast searching revealed at least 1 unique peptide
260 sequence per protein, with average sequence coverage of 26.5% (ranging from 1-89%). These
261 annotations correspond to 35 unique proteins with a number of protein isomers detected as indicated
262 by varying estimated pI (Table 2). Surprisingly, the only BPI3V related protein significantly altered
263 was Phosphoprotein P (9 isomers with isoelectric points ranging from pI 5.2 to 5.9). However,
264 other BPI3V proteins may have be present but did not pass marker selection criteria (FC > 1.5, $p <$
265 0.05 and high spot volume for MS/MS) or were poorly resolved membrane proteins
266 (haemagglutinin neuraminidase and fusion glycoprotein) a known limitation of 2D GE. This
267 protein was observed to be the second most abundant protein within cells at 48hrs p.i. (Figure 1),
268 with only actin having a slightly higher spot volume. Furthermore, gel spots corresponding to T-
269 complex proteins 1 subunit theta and 14-3-3 protein were significantly up-regulated in BPI3V
270 infected cells during the latter stages of infection (48hrs p.i.) with high intracellular abundance
271 (Figure 1D). There was a significant ($p<0.001$) correlation between the estimated and database
272 protein pI (R^2 = 0.9887) and MW (R^2 = 0.875) values for spots characterised by LC-MS,
273 confirming reliability in the identities conferred on selected proteins.

274

275 **Functional classification of differentially expressed markers of *in vitro* BPI3V infection**

276 Table 2 illustrates the functional classification, biological process and subcellular location of
277 identified proteins determined using the Gene Ontology tools PantherDB and AMIGO. The
278 proportional subcellular location of all differentially expressed proteins in FCL cells following

BPI3V infection is illustrated in Figure 2A. The majority of proteins were associated with either cytoplasmic, nuclear or cytoskeletal sub-cellular locations, with a small number originating from organelles and only collagen alpha 1 found to exist in the extracellular matrix as a secretory protein.

Figure 2B&C and Figure 2D&E illustrate the biological processes and molecular functions respectively of differentially expressed proteins. The majority of up-regulated proteins are involved in metabolic, cellular and developmental processes, and on closer inspection these proteins have key roles in mRNA translation, protein synthesis and post-translational modification as well as intracellular protein transport (Table 2 and Figure 2B and D). Furthermore, the only identified proteins involved in immune system processes were heat shock proteins 27kDa and 70kDa. Down-regulated proteins were associated with a wide range of biological processes, however 33% of the molecular functions were associated with structural molecule activity and upon closer inspection of Uniprot KB annotation these proteins were involved in maintaining cellular, sub-cellular and extra-cellular structures.

Proteins which were down-regulated at 24hrs and 48hrs p.i. as a result of BPI3V infection (collagen alpha 1, Heat shock 27kDa protein 1, and PDZ and LIM domain protein 1) are involved in supporting cellular structures in stress conditions and trafficking proteins to the cytoskeleton based on Gene Ontology (GO) annotation. At 24hrs and 48hrs p.i. a number of down-regulated proteins share biological functions associated with maintenance of cell morphology (Ezrin and Lipoma Preferred Partner) and in cytoskeleton regulation (LIM and SH3 protein domain protein 1). The protein down-regulation observed in latter stages of infection is not surprising and is likely to be associated with the visible changes in cell morphology reported in BPI3V infected cells (including detachment of cell monolayers and pyknosis, loss of cilia, intracytoplasmic inclusion bodies and syncytium formation (Campbell et al., 1969). Between 24hrs to 48hrs p.i. different expression profiles were only observed for 3 proteins: Proteasome subunit alpha type-5, 14-3-3 protein theta and 60S acidic ribosomal protein p0. The proteins up-regulated as a result of BPI3V infection are involved in a number of biological processes relating to protein production translation

(Nucleophosmin, Eukaryotic translation initiation factors 2 and 6, 60S ribosonal protein p0), protein folding (T-complex protein 1 subunit theta, Protein Disulphate Isomerase A3, Tubulin Specific Chaperone E), protein modification (Proteasome subunit beta type, Proteasome subunit alpha type 5, GANAB, aspartyl aminopeptidase), and protein trafficking (Annexin) (Table 2). Furthermore, BPI3V infection resulted in an up-regulation of proteins involved in the maintenance of cell structure (Fascin, Lamin A/C, Moesin, L-caldesmon, non-muscle myosin heavy chain, calponin-3) and cell signalling (14-3-3 protein beta/alpha/theta, cystathionine gamma lyase, osteoclast stimulating factor 1). Finally, up-regulated isocitrate dehydrogenase and 6-phosphogluconolactonase catalyse the reactions that produce NADPH and NADH, which are necessary for a number of reducing reactions such as post-translational protein modification (Smolkova and Jezek, 2012). Taken, these altered protein relationships in response to infection may reflect the exploitation of the host cell to aid the replication of viral proteins and transport to the cell membrane for budding.

Quantification of selected protein markers of *in vitro* BPI3V infection within plasma of BPI3V challenged animals

Targeted proteomic analysis was performed to assess changes in the levels of Phosphoprotein P, 14-3-3 protein beta/alpha and T-complex protein subunit theta as these are proteins found in high abundance during the latter stages of infection by proteomic analysis of *in vitro* infected cells and have the potential to be released from infected tissues into circulating biofluids. Yeast ADH loading controls demonstrated low variability (CV=11.6 and excellent recovery (96%) following SPE and no significant differences in spiked ADH levels were observed between vaccinated and non-vaccinated animals at any stage throughout the study. Proteotypic peptides for Phosphoprotein P and T-complex protein subunit theta were detected and quantified within plasma at days 0, 1, 2, 5, 6, 14 and 20 post-BPI3V challenge in both vaccinated and non-vaccinated study groups. However, no peptides corresponding to 14-3-3 protein beta/alpha were detectable in plasma at any time point.

331 Unique peptides for phosphoprotein P and T-complex protein 1 subunit theta were found to be
332 significantly ($p<0.05$) up-regulated at day 5 p.i. in non-vaccinated animals compared to vaccinated
333 animals at the same stage as illustrated in Figure 3. Plasma levels of Phosphoprotein P (Figure 3A)
334 were found to increase significantly ($p<0.05$) from day 1 to day 5 post-BPI3V challenge in non-
335 vaccinated animals.
336
337

Discussion

Lysates obtained from mock and BPI3V infected FCL cells were profiled by 2D Gel Electrophoresis to assess host cell proteome responses to BPI3V infection and identify potential *in vivo* infection markers of diagnostic potential. 57 proteins spots were significantly altered in FCL cells as a result of BPI3V infection, corresponding to 35 unique protein identifications. Whilst to date there are no reports relating the effects of BPI3V infection on the intracellular proteome or the proteomic effects of paramyxoviruses on respiratory fibroblasts, intracellular proteomic responses to Human Parainfluenza Virus-3 (hPIV-3) (van Diepen et al., 2010) and Respiratory Syncytial Virus (RSV) (Brasier et al., 2004, Munday et al., 2010, van Diepen et al., 2010, Hastie et al., 2012, Ternette et al., 2011) infections have been investigated. Such studies have reported similar findings to the current investigation, with an up-regulation of lamin A/C (van Diepen et al., 2010) 20, 22], nucleophosphim (van Diepen et al., 2010), protein disulphate isomerase A3 (PDIA3) (Hastie et al., 2012), indicating host-cell immune responses to BPI3V infection - as PDIA3 mediates MCH class I peptide presentation and lamin A/C represses viral replication (Mou et al., 2008). In A549 respiratory epithelial cells paramyxovirus infection resulted in an up-regulation of host-proteins linked to apoptotic processes and a shut-down of transcription, RNA processing and protein biosynthesis (van Diepen et al., 2010, Munday et al., 2010). However, this study's findings indicate that BPI3V does not induce complete shut-down of host protein synthesis or apoptosis in fibroblasts, resulting in virus-host mRNA competition for virus propagation. Fibroblast pro-inflammatory response to UV inactivated virus has been observed due to stress mediators present in HeLa propagation cultures (Bedke et al., 2009, Oliver et al., 2006), however, no such pro-inflammatory response was observed in this study. As FCL fibroblasts were employed for BPI3V propagation the model system for biomarker screening employed closely reflects that which occurs in vivo - i.e. the presence of not only virus induced protein changes but also the stress response from surrounding tissue sites. Furthermore, any stress response markers produced during viral replication should closely match the *in vivo* response within the lung interstitium, and therefore as a

364 model of determining BPI3V candidate markers this study closely matches *in vivo* conditions in
365 specific tissue regions. An increase in the levels of proteins associated with RNA translation,
366 protein folding and post-translational-modification were observed in BPI3V infected fibroblasts.
367 Up-regulated annexin A11, previously observed inside influenza virions (Shaw et al., 2008) and
368 thought to play a role in virus assembly, could be assisting trafficking of viral proteins to the plasma
369 membrane and budding. These observations suggest that fibroblasts respond to BPI3V infection by
370 increasing the production of proteins to combat the competitive effects of viral mRNA and the
371 associated demand for protein folding and protein modification. Furthermore, the down-regulation
372 of key intra- and extra-structural proteins reflects how BPI3V infection induces changes in cell
373 morphology.

374 Phosphoprotein P, T-complex protein 1 subunit theta and 14-3-3 protein beta/alpha, levels
375 of which were significantly increased within BPI3V infected FCL cells, were selected as potential
376 diagnostic markers of *in vivo* BPI3V infection. Whilst other proteins involved in anti-viral immune
377 response mechanisms were significantly altered in BPI3V infected cells (e.g Lamin A/C and
378 PDIA3) they were not selected due to lower intracellular abundance and associated reduced chance
379 for detection in circulating bio-fluids. Phosphoprotein P is involved in the assembly of viral RNA
380 polymerase complex and is associated with intracellular defence avoidance (Gale and Katze, 1998)
381 through shutdown of host cell protein production (Gainey et al., 2008, Komatsu et al., 2007).
382 Transcriptional activity of BPI3V proteins is highest at 3' region, and as Phosphoprotein P occurs in
383 the second ORF (Vainionpää and Hyypiä, 1994), its expression is elevated relative to other BPI3V
384 viral proteins. A high intracellular abundance of Phosphoprotein P has been reported previously in
385 studies performing 2D GE investigations of other paramyxoviruses (Hastie et al., 2012). However,
386 within virions Phosphoprotein P represents only a small proportion of total protein (Ellis, 2010),
387 and a significant quantity of free Phosphoprotein P may not be encapsulated within budding virions.
388 A high level of free Phosphoprotein P may therefore be released into the circulatory system as
389 infected cells die making it detectable as a marker of tissue death. Such diagnostic approaches

390 based on proteins released from infected cells have previously been employed for Dengue and
391 West-Nile Virus (Alcon et al., 2002, Yeh et al., 2012), enabling rapid identification of infected
392 individuals prior to antibody response and differentiation of live virus antibody responses from
393 inactivated virus vaccines. Molecular chaperone T-complex protein 1 subunit theta and
394 signalling/binding protein 14-3-3 protein beta/alpha were also found to be accumulated within cells
395 at the latter stages of *in vitro* infection, and might be candidate markers of tissue damage *in vivo*.

396 Targeted multiple-reaction-monitoring (MRM) tandem mass spectrometry (MS/MS)
397 analysis was performed to determine the presence or otherwise of proteins identified through *in*
398 *vitro* analysis within plasma of vaccinated and non-vaccinated animals challenged with BPI3V and
399 to assess their potential as diagnostic markers of *in vivo* infection. Unique peptides corresponding to
400 Phosphoprotein P and T-complex protein 1 subunit theta were detected in bovine plasma, however
401 14-3-3 protein beta/alpha could not be detected. Levels of Phosphoprotein P and T-complex protein
402 1 subunit theta were significantly up-regulated in non-vaccinated animals compared to those
403 vaccinated at day 5 post BPI3V challenge. Peak BPI3V titre *in vivo* has been demonstrated to occur
404 between days 4 to 6 p.i., and furthermore, vaccinated animals respond quicker, clearing the
405 infections rapidly (Xue et al., 2010). In particular for Phosphoprotein P, increasing levels in non-
406 vaccinated animals from day 0 to day 5 p.i. compared to vaccinated animals, mirrors that of viral
407 shedding observed in vaccinated animals compared to non-vaccinated, i.e. virus titre peaking at
408 days 4-6 p.i. in non-vaccinated animals and days 1-2 p.i. in vaccinated animals (Xue et al., 2010).
409 This is not surprising as when more infected cells die, increased levels of intracellularly
410 accumulated Phosphoprotein P and T-complex protein 1 subunit theta will be released into the
411 circulation. However, the levels of both these proteins dropped from day 5 to 6 post-BPI3V
412 challenge in non-vaccinated animals. These findings indicate that it is possible that these proteins
413 are rapidly degraded in the circulation and although their presence in plasma is an indicator of a
414 specific virus induced damage to the respiratory tract there may be a limited window for their useful
415 diagnostic application.

In conclusion, this study has demonstrated that proteomic analysis of BPI3V infection *in vitro* is capable of identifying protein infection markers, which subsequently are detectable in plasma of animals following BPI3V infection. BPI3V induced alterations to the intracellular proteome of respiratory fibroblasts resulted in elevated levels of host-proteins associated with mRNA translation, protein translation, post-translational modification and cellular protein trafficking. Viral (Phosphoprotein P) and host (T-complex protein 1 subunit theta) proteins accumulated intracellularly during the latter stages of infection may be released into the circulation, and elevated levels were found to occur in plasma of non-vaccinated BPI3V challenged animals at periods associated with peak virus titre. Compared to serological ELISA, which relies on the measurement of a single parameter (antibodies), assessment of such protein markers would provide increased information on the health status of pre-convalescent animals during infection outbreaks, or verify absence of sub-clinical disease in those identified as seropositive. Further research is needed to validate these markers on a larger scale and to develop more applicable diagnostic tests which can quantify protein levels in routine analysis. The utilisation of such markers diagnostically would improve disease management decisions through the identification of animals undergoing active BPIV3 infection and the presence of necrotic tissue, a major risk factor for the development of more severe bacterial pneumonia. Such a proteomic approach to the identification of markers of infection may also be relevant to other viruses which persist for longer periods within hosts offering longer useful diagnostic windows.

Acknowledgements

This research was funded by a Department of Agriculture and Rural Development (DARD) Northern Ireland postgraduate studentship awarded to Darren Gray.

441 **References**

442 1. AFBI/DAFM. 2012. All-island Animal Disease Surveillance Report 2011 [Online].
443 AFBI/DAFM Veterinary Laboratories. Available: http://www.afbini.gov.uk/all-
444 island_animal_disease_surveillance_report_2011reduced.pdf [Accessed 24 September 2013].

445 2. ALCON, S., TALARMIN, A., DEBRUYNE, M., FALCONAR, A., DEUBEL, V. &
446 FLAMAND, M. 2002. Enzyme-linked immunosorbent assay specific to dengue virus type 1
447 nonstructural protein NS1 reveals circulation of the antigen in the blood during the experiencing
448 primary acute phase of disease in patients or secondary infections. Journal of Clinical
449 Microbiology, 40, 376-381.

450 3. ANDERSON, N. L., ESQUERBLASCO, R., HOFMANN, J. P., MEHEUS, L.,
451 RAYMACKERS, J., STEINER, S., WITZMANN, F. & ANDERSON, N. G. 1995. ART
452 UPDATED 2-DIMENSIONAL GEL DATABASE OF RAT-LIVER PROTEINS USEFUL IN
453 GENE-REGULATION AND DRUG EFFECT STUDIES. Electrophoresis, 16, 1977-1981.

454 4. BAKER, J. C., ELLIS, J. A. & CLARK, E. G. 1997. Bovine respiratory syncytial virus.
455 Veterinary Clinics of North America-Food Animal Practice, 13, 425-454.

456 5. BEDKE, N., HAITCHI, H. M., XATZIPSALTI, M., HOLGATE, S. T. & DAVIES, D. E.
457 2009. Contribution of bronchial fibroblasts to the antiviral response in asthma. J Immunol, 182,
458 3660-7.

459 6. BRASIER, A. R., SPRATT, H., WU, Z., BOLDOGH, I., ZHANG, Y. H., GAROFALO, R.
460 P., CASOLA, A., PASHMI, J., HAAG, A., LUXON, B. & KUROSKY, A. 2004. Nuclear heat
461 shock response and novel nuclear domain 10 reorganization in respiratory syncytial virus-infected
462 A549 cells identified by high-resolution two-dimensional gel electrophoresis. Journal of Virology,
463 78, 11461-11476.

464 7. BRYSON, D. G. 1985. CALF PNEUMONIA. Veterinary Clinics of North America-Food
465 Animal Practice, 1, 237-257.

8. CAMPBELL, R. S. F., THOMPSON, H., LEIGHTON, E. & PENNY, W. 1969. PATHOGENESIS OF BOVINE PARAINFLUENZA 3 VIRUS INFECTION IN ORGAN CULTURES. Journal of Comparative Pathology, 79, 347-354.

9. CRASTO, C., NARNE, C., KAWAI, M., WILSON, L. & BARNES, S. 2013. MRMPath and MRMutation, Facilitating Discovery of Mass Transitions for Proteotypic Peptides in Biological Pathways Using a Bioinformatics Approach. Advances in bioinformatics, 2013, 527295.

10. CUSACK, P. M. V., MCMENIMAN, N. & LEAN, I. J. 2003. The medicine and epidemiology of bovine respiratory disease in feedlots. Australian Veterinary Journal, 81, 480-487.

11. ELLIS, J. 2010. Bovine Parainfluenza-3 Virus. The veterinary clinics of North America. Food animal practice, 26, 575-593.

12. FULTON, R. W. & CONFER, A. W. 2012. Laboratory test descriptions for bovine respiratory disease diagnosis and their strengths and weaknesses: Gold standards for diagnosis, do they exist? Canadian Veterinary Journal-Revue Veterinaire Canadienne, 53, 754-761.

13. GAINEY, M. D., DILLON, P. J., CLARK, K. M., MANUSE, M. J. & PARKS, G. D. 2008. Paramyxovirus-induced shutoff of host and viral protein synthesis: Role of the P and V proteins in limiting PKR activation. Journal of Virology, 82, 828-839.

14. GALE, M. & KATZE, M. G. 1998. Molecular mechanisms of interferon resistance mediated by viral-directed inhibition of PKR, the interferon-induced protein kinase. Pharmacology & Therapeutics, 78, 29-46.

15. GRAY, D. W., WELSH, M. D., DOHERTY, S., MANSOOR, F., CHEVALLIER, O. P., ELLIOTT, C. T. & MOONEY, M. H. 2015. Identification of systemic immune response markers through metabolomic profiling of plasma from calves given an intra-nasally delivered respiratory vaccine. Veterinary Research, 46, 16.

16. GRIFFIN, D. 1997. Economic impact associated with respiratory disease in beef cattle. Veterinary Clinics of North America-Food Animal Practice, 13, 367-&.

17. HASTIE, M. L., HEADLAM, M. J., PATEL, N. B., BUKREYEV, A. A., BUCHHOLZ, U. J., DAVE, K. A., NORRIS, E. L., WRIGHT, C. L., SPANN, K. M., COLLINS, P. L. & GORMAN, J. J. 2012. The Human Respiratory Syncytial Virus Nonstructural Protein 1 Regulates Type I and Type II Interferon Pathways. Molecular & Cellular Proteomics, 11, 108-127.

18. KAHRS, R. F. 2001. Viral Diseases Of Cattle, Iowa, Iowa State University Press.

19. KAPIL, S. & BASARABA, R. J. 1997. Infectious bovine rhinotracheitis, parainfluenza-3, and respiratory coronavirus. Veterinary Clinics of North America-Food Animal Practice, 13, 455-469.

20. KINKEAD, R. A., ELLIOTT, C. T., CANNIZZO, F. T., BIOLATTI, B. & MOONEY, M. H. 2015. Proteomic identification of plasma proteins as markers of growth promoter abuse in cattle. Analytical and Bioanalytical Chemistry, 407, 4495-4507.

21. KOMATSU, T., TAKEUCHI, K. & GOTOH, B. 2007. Bovine parainfluenza virus type 3 accessory proteins that suppress beta interferon production. Microbes and Infection, 9, 954-962.

22. MACLEAN, B., TOMAZELA, D. M., SHULMAN, N., CHAMBERS, M., FINNEY, G. L., FREWEN, B., KERN, R., TABB, D. L., LIEBLER, D. C. & MACCOSS, M. J. 2010. Skyline: an open source document editor for creating and analyzing targeted proteomics experiments. Bioinformatics, 26, 966-968.

23. MOU, F., WILLS, E. G., PARK, R. & BAINES, J. D. 2008. Effects of lamin A/C, lamin B1, and viral U(s)3 kinase activity on viral infectivity, virion egress, and the targeting of herpes simplex virus U(L)34-Encoded protein to the inner nuclear membrane. Journal of Virology, 82, 8094-8104.

24. MUNDAY, D. C., EMMOTT, E., SURTEES, R., LARDEAU, C.-H., WU, W., DUPREX, W. P., DOVE, B. K., BARR, J. N. & HISCOX, J. A. 2010. Quantitative Proteomic Analysis of A549 Cells Infected with Human Respiratory Syncytial Virus. Molecular & Cellular Proteomics, 9, 2438-2459.

516 25. OLIVER, B. G., JOHNSTON, S. L., BARAKET, M., BURGESS, J. K., KING, N. J.,
517 ROTH, M., LIM, S. & BLACK, J. L. 2006. Increased proinflammatory responses from asthmatic
518 human airway smooth muscle cells in response to rhinovirus infection. Respir Res, 7, 71.
519 26. RUBPORN, A., SRISOMSAP, C., SUBHASITANONT, P., CHOKCHAICHAMNANKIT,
520 D., CHIABLAEM, K., SVASTI, J. & SANGVANICH, P. 2009. Comparative Proteomic Analysis
521 of Lung Cancer Cell Line and Lung Fibroblast Cell Line. Cancer Genomics & Proteomics, 6, 229-
522 237.
523 27. SHAW, M. L., STONE, K. L., COLANGELO, C. M., GULCICEK, E. E. & PALESE, P.
524 2008. Cellular proteins in influenza virus particles. Plos Pathogens, 4.
525 28. SHEPHARD, M. J., TODD, D., ADAIR, B. M., PO, A. L. W., MACKIE, D. P. & SCOTT,
526 E. M. 2003. Immunogenicity of bovine parainfluenza type 3 virus proteins encapsulated in
527 nanoparticle vaccines, following intranasal administration to mice. Research in Veterinary Science,
528 74, 187-190.
529 29. SHEVCHENKO, A., TOMAS, H., HAVLIS, J., OLSEN, J. V. & MANN, M. 2006. In-gel
530 digestion for mass spectrometric characterization of proteins and proteomes. Nature Protocols, 1,
531 2856-2860.
532 30. SMOLKOVA, K. & JEZEK, P. 2012. The Role of Mitochondrial NADPH-Dependent
533 Isocitrate Dehydrogenase in Cancer Cells. International journal of cell biology, 2012, 273947-
534 273947.
535 31. TERNETTE, N., WRIGHT, C., KRAMER, H. B., ALTUN, M. & KESSLER, B. M. 2011.
536 Label-free quantitative proteomics reveals regulation of interferon-induced protein with
537 tetratricopeptide repeats 3 (IFIT3) and 5 '-3 '-exoribonuclease 2 (XRN2) during respiratory
538 syncytial virus infection. Virology Journal, 8.
539 32. TRIGO, E., LIGGITT, H. D., EVERMANN, J. F., BREEZE, R. G., HUSTON, L. Y. &
540 SILFLOW, R. 1985. EFFECT OF INVITRO INOCULATION OF BOVINE RESPIRATORY

SYNCYTIAL VIRUS ON BOVINE PULMONARY ALVEOLAR MACROPHAGE FUNCTION. American Journal of Veterinary Research, 46, 1098-1103.

33. VAINIONPÄÄ, R. & HYYPIÄ, T. 1994. Biology of parainfluenza viruses. Clin Microbiol Rev, 7, 265-75.

34. VAN DIEPEN, A., BRAND, H. K., SAMA, I., LAMBOOY, L. H. J., VAN DEN HEUVEL, L. P., VAN DER WELL, L., HUYNEN, M., OSTERHAUS, A., ANDEWEG, A. C. & HERMANS, P. W. M. 2010. Quantitative proteome profiling of respiratory virus-infected lung epithelial cells. Journal of Proteomics, 73, 1680-1693.

35. VAUCHER, R. D., SIMONETTI, A. B. & ROEHE, P. M. 2008. RT-PCR for detection of bovine parainfluenza virus type 3 (bPIV-3). Acta Scientiae Veterinariae, 36, 215-220.

36. XUE, W. Z., ELLIS, J., MATTICK, D., SMITH, L., BRADY, R. & TRIGO, E. 2010. Immunogenicity of a modified-live virus vaccine against bovine viral diarrhea virus types 1 and 2, infectious bovine rhinotracheitis virus, bovine parainfluenza-3 virus, and bovine respiratory syncytial virus when administered intranasally in young calves. Vaccine, 28, 3784-3792.

37. YEH, J. Y., CHUNG, K. M. & SONG, J. 2012. Differentiation of West Nile Virus-Infected Animals from Vaccinated Animals by Competitive ELISA Using Monoclonal Antibodies Against Non-Structural Protein 1. Vector-Borne and Zoonotic Diseases, 12, 380-387.

Table 1: LC-MS identification of 2D GE spots from BPI3V infected FCL cells at 24hr and 48hrs p.i. Spots were excised from coomassie stained gels and analysed by LC-MS using Thermo XL Orbitrap coupled to a Dionex HPLC system. Spectra were imported into Peaks Studio (version 6), de novo sequenced and analysed against a combined UniprotKB *Bos Taurus* and BPI3V sequence database for the identification. Spots were matched based on MW and pI calibration from gels. FC = fold change, p = significance (one-way ANOVA).

Table 2: Classification of biological processes, molecular functions and subcellular locations of the identified differentially expressed proteins. The Panther database (version 8.1, http://www.pantherdb.org/) was used for functional classification of identified proteins. Where functional classification could not be determined using Panther, AmiGO (version 1.8, http://amigo.geneontology.org/cgi-bin/amigo/go.cgi) experimental evidence code gene ontology annotations were selected. Subcellular location was determined from Uniprot KB annotation. As

572 the bovine reference database is small, where annotation was not possible human homologues
573 substituted.

574

Figure 1: Representative images of control and BPI3V infected FCL cells at 24hrs and 48hrs p.i. Cell lysates from (A) control, (B) 24hr post-BPI3V infection and (C) 48hr post-BPI3V infection FCL cells were analysed by 2D Gel Electrophoresis using 13cm pH 3-10 NL IPG strips in the first dimension and 12.5% SDS-PAGE lab cast gels in the second dimension. Gels were scanned using an Epson v750 Pro scanner and spot matching, warping and statistical analysis performed using Ludesi Redfin. Differentially expressed protein spots are indicated with circles on each gel. (D) The 3D spots for the proteins 14-3-3protein beta/alpha, Phosphoprotein P and T-complex protein 1 subunit theta at each sampling point are indicated. Gel image adjustments were performed automatically by Ludesi Redfin.

Figure 2: Subcellular location, biological processes and molecular function of differentially expressed FCL cell proteins as a result of BPI3V infection. Subcellular location, was determined from UniprotKB annotation for the proteins selected by 2D GE and identified by LC-MS. Biological processes and molecular function was determined from Gene Ontology analysis performed using Panther DB (and AMIGO where no annotation was available). As the bovine reference database is small, where annotation of subcellular location was not possible human homologues substituted.

Figure 3: Quantification of Phosphoprotein P and T-Complex Protein 1 Subunit Theta markers for BPI3V infection by UPLC-MS/MS. At day 0-6 p.i. (n=6) and day 14-20 p.i.(n=3). Values represent mean ± S.E.M. Relative quantification of the peptide markers was performed by interpolating the average peptide intensity (integrated peptide area) and normalizing against trypsin auto digestion products (fixed volume of trypsin per sample added prior to C18 SPE) to account for variations in recovery.

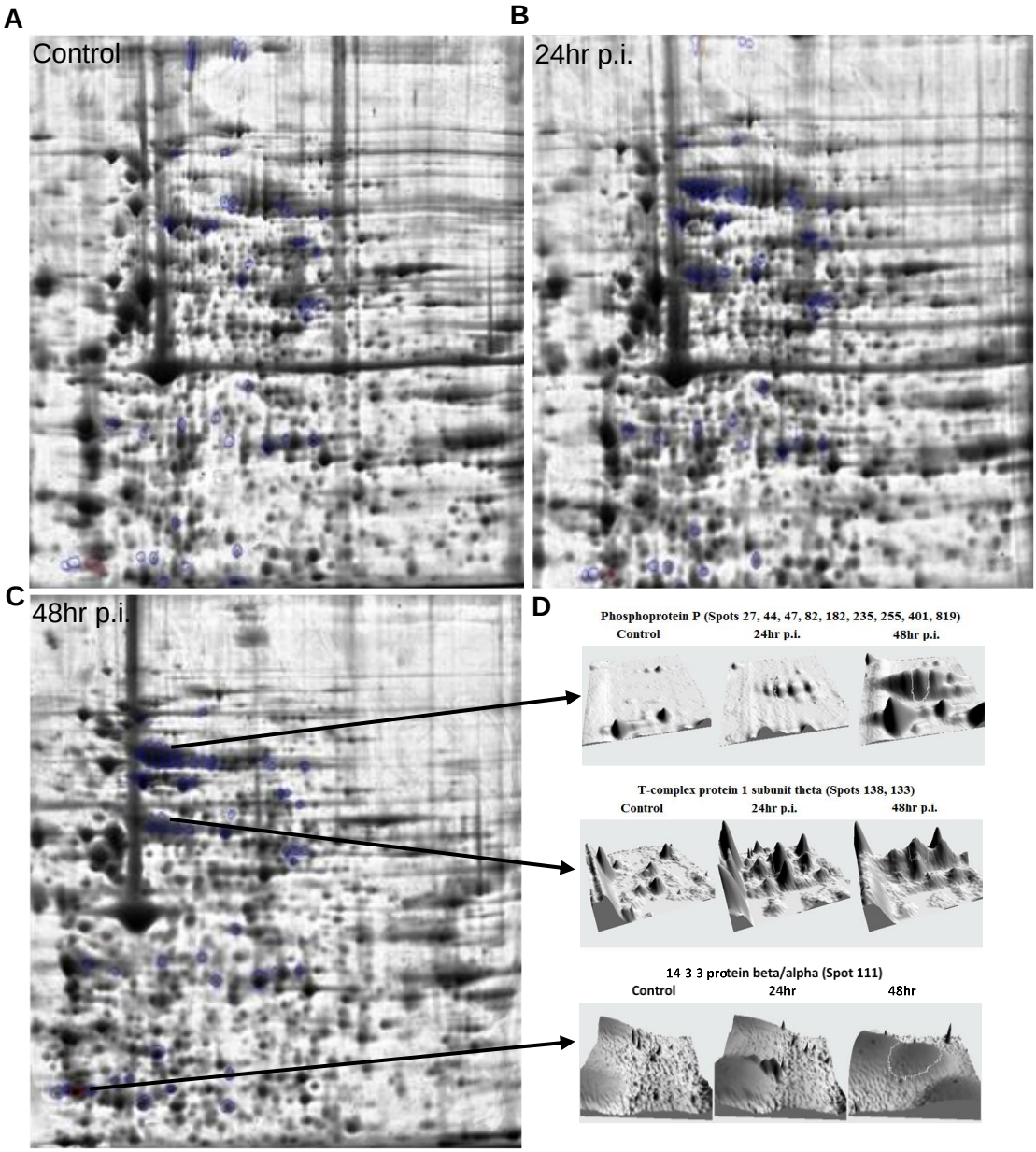
A
Control
B
24hr p.i.
C
48hr p.i.
D
Phosphoprotein P (Spots 27, 44, 47, 82, 182, 235, 255, 401, 819)
Control
24hr p.i.
48hr p.i.
T-complex protein 1 subunit theta (Spots 138, 133)
Control
24hr p.i.
48hr p.i.
14-3-3 protein beta/alpha (Spot 111)
Control
24hr
48hr

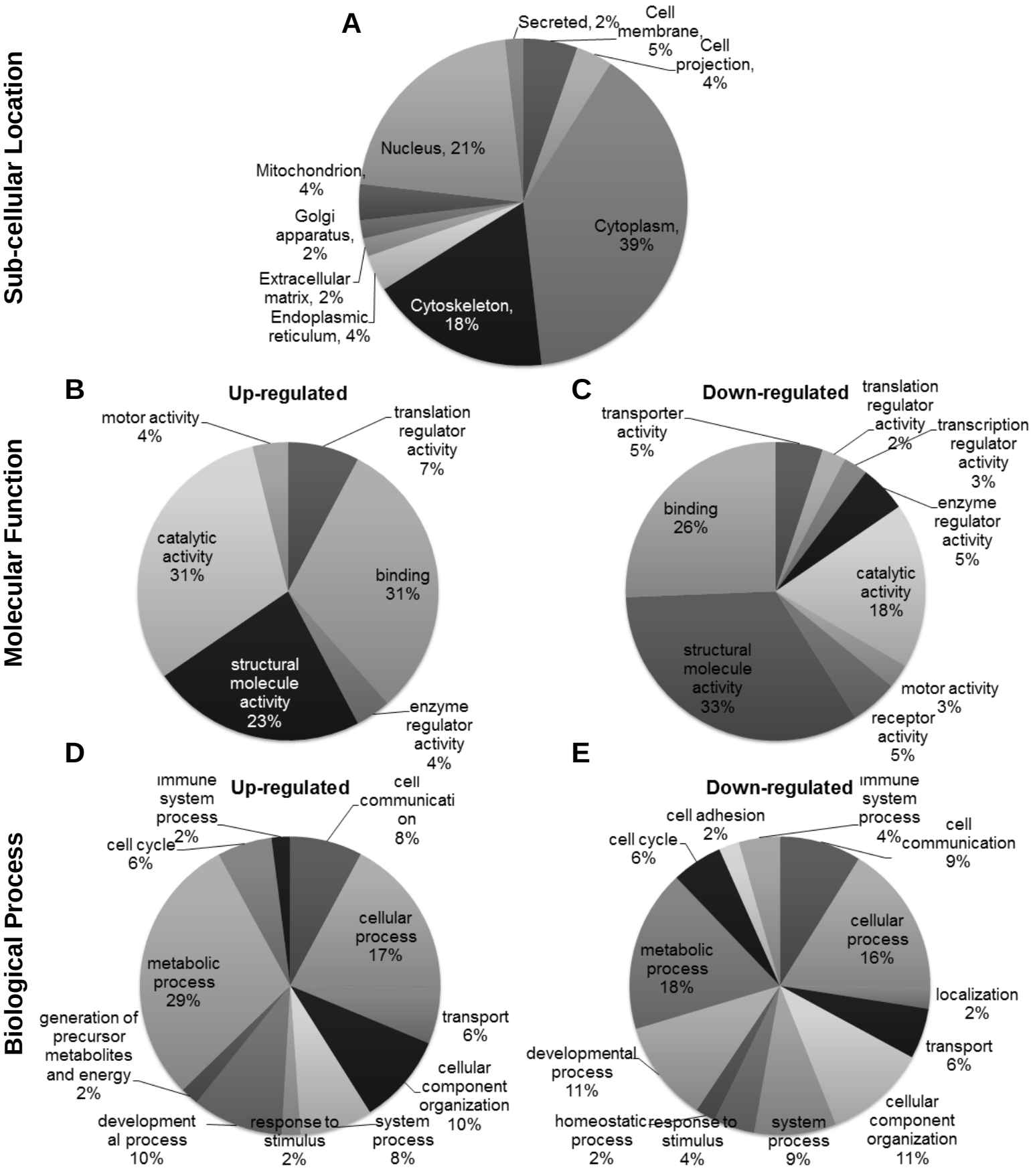
Sub-cellular Location
A
Secreted, 2%
Cell membrane, 5%
Cell projection, 4%
Nucleus, 21%
Mitochondrion, 4%
Golgi apparatus, 2%
Extracellular matrix, 2%
Endoplasmic reticulum, 4%
Cytoplasm, 39%
Cytoskeleton, 18%
Molecular Function
B
Up-regulated
motor activity 4%
translation regulator activity 7%
catalytic activity 31%
binding 31%
structural molecule activity 23%
enzyme regulator activity 4%
C
Down-regulated
transporter activity 5%
translation regulator activity 2%
transcription regulator activity 3%
enzyme regulator activity 5%
binding 26%
catalytic activity 18%
structural molecule activity 33%
motor activity 3%
receptor activity 5%
Biological Process
D
Up-regulated
immune system process 2%
cell communication 8%
cell cycle 6%
cellular process 17%
metabolic process 29%
transport 6%
generation of precursor metabolites and energy 2%
cellular component organization 10%
development al process 10%
response to stimulus 2%
system process 8%
E
Down-regulated
immune system process 4%
cell adhesion 2%
cell communication 9%
cell cycle 6%
cellular process 16%
metabolic process 18%
localization 2%
transport 6%
developmental process 11%
cellular component organization 11%
homeostatic process 2%
response to stimulus 4%
system process 9%

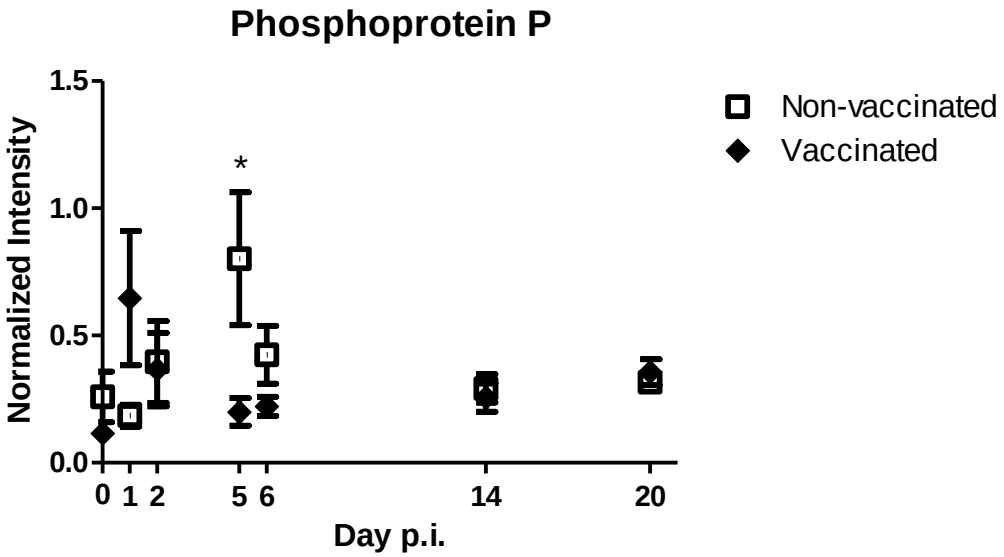
Phosphoprotein P
Normalized Intensity
1.5
1.0
0.5
0.0
*
0 1 2 5 6 14 20
Day p.i.
Non-vaccinated
Vaccinated

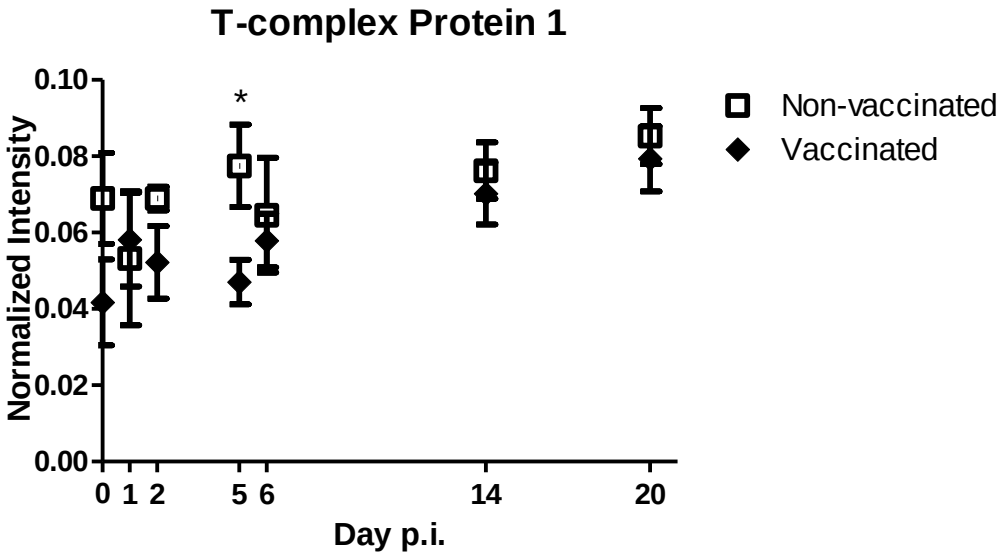
T-complex Protein 1
Normalized Intensity
0.10
0.08
0.06
0.04
0.02
0.00
*
0 1 2 5 6 14 20
Day p.i.
Non-vaccinated
Vaccinated

Description	Uniprot I.D	Spot ID	Estimated		Database Identification							Comparison to control			
												24hr p.i.		48hr p.i.	
			MW (Da)	pI	MW (Da)	pI	Accession	-10lgP	Coverage (%)	# Peptides	# Unique	FC	p	FC	p
Collagen alpha-1(III) chain	F1MXS8_BOVIN	358	139000	6.20	138928	6.32	F1MXS8_BOVIN	215.04	8	11	11	-18.19	1.15E-02	-38.36	1.03E-02
		415	139000	6.10			F1MXS8_BOVIN	222.76	6	8	8	-15.41	1.07E-02	-38.53	9.37E-03
Collagen alpha-1(I) chain	CO1A1_BOVIN	210	138300	5.60	138939	5.60	CO1A1_BOVIN	209.49	10	14	14	-7.94	1.50E-02	-19.58	1.12E-02
		359	138200	5.50			CO1A1_BOVIN	194.18	8	12	12	-4.23	2.05E-03	-6.00	1.22E-03
Heat shock 27kDa protein 1	E9RHW1_BOVIN	42	23700	6.00	22393	5.98	E9RHW1_BOVIN	221.6	89	26	26	-3.08	1.58E-02	-2.63	2.14E-02
PDZ and LIM domain 1	A6H7E3_BOVIN	509	37600	6.80	35821	6.76	A6H7E3_BOVIN	78.37	6	2	2	-2.08	3.41E-02	-3.37	1.27E-02
Lipoma-preferred partner	E1BMD6_BOVIN	82	66600	7.70	65715	7.44	E1BMD6_BOVIN	61.6	2	1	1			-3.56	8.55E-03
LIM and SH3 domain protein 1	LASP1_BOVIN	102	31600	7.60	29677	7.07	LASP1_BOVIN	115.59	14	4	4			-3.21	4.19E-03
Ezrin	EZRI_BOVIN	264	68000	6.30	68760	6.07	EZRI_BOVIN	171.82	19	13	13			-3.98	8.54E-03
Proteasome subunit alpha type-5	PSA5_BOVIN	185	25900	4.70	26411	4.74	PSA5_BOVIN	71.4	5	1	1	-2.04	4.08E-02	5.36	1.75E-02
14-3-3 protein theta	1433T_BOVIN	2	27000	4.60	27764	4.80	1433T_BOVIN	80.11	21	7	4	-1.95	4.84E-03	14.85	1.13E-02
60S acidic ribosomal protein P0	RLA0_BOVIN	338	34000	6.00	34371	5.70	RLA0_BOVIN	204.13	31	8	8	-1.76	3.72E-02	2.01	3.22E-02
Aspartyl aminopeptidase	DNPEP_BOVIN	132	51700	7.50	51828	6.45	DNPEP_BOVIN	207.84	27	10	10	1.52	4.55E-02		
Fascin	Q3MHK9_BOVIN	125	54100	6.60	54785	6.50	Q3MHK9_BOVIN	269.33	49	29	29	1.69	1.68E-02		
Lamin A/C	Q3SZI2_BOVIN	79	63000	6.80	65122	6.54	Q3SZI2_BOVIN	192.44	27	17	17	2.13	3.24E-02		
GANAB protein	A6QNJ8_BOVIN	330	90000	5.80	109085	5.74	A6QNJ8_BOVIN	158.36	11	12	12	2.01	2.29E-02		
Tubulin-specific chaperone E	TBCE_BOVIN	458	61200	6.20	59327	5.97	TBCE_BOVIN	177.65	21	11	11	2.13	1.28E-02		
Serine hydroxymethyltransferase	GLYM_BOVIN	419	55000	7.70	55606	6.51	GLYM_BOVIN	302.28	53	24	24	2.29	1.32E-03		
Annexin A11	ANX11_BOVIN	227	55000	7.70	54018	7.53	ANX11_BOVIN	194.76	34	17	17	1.96	1.36E-02		
Moesin	MOES_BOVIN	318	66500	6.00	67975	5.91	MOES_BOVIN	138.2	11	9	9	1.75	3.51E-03	1.73	9.37E-03
Eukaryotic translation initiation factor 2 subunit 1	F2A_BOVIN	573	36000	4.80	36108	5.02	F2A_BOVIN	217.29	29	10	10	1.76	2.91E-02	2.30	3.00E-03
L-caldesmon	Q8HYY3_BOVIN	110	67800	6.10	62086	6.24	Q8HYY3_BOVIN	232.35	29	17	17	1.63	1.20E-02	1.84	6.81E-04
Osteoclast-stimulating factor 1	OSTF1_BOVIN	40	23700	5.20	23842	5.30	OSTF1_BOVIN	129.72	15	3	3	2.74	7.81E-05	10.08	7.84E-03
T-complex protein 1 subunit theta	TCPQ_BOVIN	138	57900	5.40	59610	5.39	TCPQ_BOVIN	165.76	12	7	7	5.37	2.62E-06	14.22	2.59E-03
	TCPQ_BOVIN	133	58300	5.40	59610		TCPQ_BOVIN	259.08	39	19	19	2.85	5.23E-03	10.72	1.10E-02
BPI3V Phosphoprotein P	E5LP67_PI3B	27	68100	5.20	67770		E5LP67_PI3B	317.64	35	29	19	8.73	8.76E-05	43.66	1.63E-03
	E5LP67_PI3B	182	68200	5.70	67770		E5LP67_PI3B	235.92	28	19	1	12.89	3.45E-05	19.22	9.17E-03
	E5LP67_PI3B	92	68100	5.60	67770		E5LP67_PI3B	330.89	46	34	5	13.91	1.55E-03	32.23	1.90E-03
	E5LP67_PI3B	44	68000	5.30	67710		L0HCM6_PI3B	258.68	27	18	0	17.79	4.97E-05	70.50	1.91E-03
	E5LP67_PI3B	47	68000	5.40	67770	5.58	E5LP67_PI3B	356.71	37	30	21	39.26	1.62E-04	115.92	1.88E-03
	B2C5X6_PI3B	401	67100	5.70	66460		B2C5X6_PI3B	200.25	13	8	1	52.55	1.25E-04	142.08	7.15E-03
	E5LP67_PI3B	819	67700	5.20	67770		E5LP67_PI3B	308.16	47	35	5	4.16	3.77E-04	30.94	1.57E-02
	E5LP67_PI3B	255	67400	5.90	67710		L0HCM6_PI3B	61.73	1	1	1	1.57	3.42E-02	2.28	2.75E-04
	E5LP67_PI3B	235	68100	5.80	67770		E5LP67_PI3B	248.51	25	15	15	2.70	1.46E-04	4.02	1.96E-04
Protein disulfide-isomerase A3	A5D7E8_BOVIN	333	58000	5.70	56930	5.78	PDIA3_BOVIN	76.9	6	3	3	2.08	8.76E-03	13.32	1.26E-02
	A5D7E8_BOVIN	25	56800	6.40	56930		A5D7E8_BOVIN	347	62	42	42			2.93	2.35E-02
Annexin	I6YIV1_BOVIN	16	37300	6.30	38992	6.37	I6YIV1_BOVIN	309.26	62	27	27			2.95	7.07E-03
Non-muscle myosin heavy chain	O02717_BOVIN	48	72400	5.20	72371	5.02	O02717_BOVIN	354.67	52	41	2			5.07	7.08E-03
Nucleophosmin	E3SAZ8_BOVIN	57	32200	4.70	32201	4.20	E3SAZ8_BOVIN	176.18	27	6	6			2.82	2.19E-02
6-phosphogluconolactonase	F1MM83_BOVIN	62	28200	5.40	27531	5.57	F1MM83_BOVIN	150.98	15	3	3			4.02	8.53E-03
14-3-3 protein beta/alpha	1433B_BOVIN	111	26600	4.70	28081	4.80	1433B_BOVIN	112.17	17	4	2			6.60	2.16E-04
Cystathionine gamma-lyase	E1BNH2_BOVIN	134	40100	6.10	44380	6.01	E1BNH2_BOVIN	153.36	22	8	8			1.29	4.97E-02
Phosphoserine phosphatase	SERB_BOVIN	158	24900	5.20	24850	5.20	SERB_BOVIN	164.75	27	6	6			2.37	1.82E-02
Heat shock 70 kDa protein	HS71B_BOVIN	5	64600	5.20	70229	5.20	HS71B_BOVIN	336.85	42	35	21			2.16	7.84E-03
	HSP7C_BOVIN	166	64900	5.20	71241		HSP7C_BOVIN	322.6	47	29	18			2.38	1.78E-02
Proteasome subunit beta type	F1MBI1_BOVIN	272	27300	6.10	29996	6.44	F1MBI1_BOVIN	169.83	34	11	11			1.58	4.63E-03
Calponin-3	CNN3_BOVIN	357	36000	5.40	36358	5.42	CNN3_BOVIN	182.15	26	7	7			1.65	1.41E-02
Isocitrate dehydrogenase [NAD] subunit alpha	IDH3A_BOVIN	481	39300	5.80	39668	5.80	IDH3A_BOVIN	77.86	5	2	2			1.68	2.99E-02
Eukaryotic translation initiation factor 6	IF6_BOVIN	532	25900	4.60	26513	4.60	IF6_BOVIN	171.54	22	4	4			3.16	1.61E-02

Description	Spot ID	Relationship to control 24hr p.i.	Relationship to control 48hr p.i.	Biological process	Molecular function	Subcellular Location
Collagen alpha-1(III) chain	**358;415**	DOWN	DOWN	Receptor activity; extracellular matrix structural constituent; transmembrane transporter activity	Macrophage activation; blood circulation;intracellular protein transport; receptor-mediated endocytosis; signal transduction; cell-cell adhesion; cellular component morphogenesis; ectoderm development; mesoderm development; skeletal system development; angiogenesis; regulation of liquid surface tension; defense response to bacterium; asymmetric protein localization	Secreted; extracellular matrix
Collagen alpha-1(I) chain	**210;359**	DOWN	DOWN			
Heat shock 27kDa protein 1	**42**	DOWN	DOWN	Structural molecule activity	Immune system process;muscle contraction; visual perception; sensory perception; protein folding; response to stress	Cytoplasm; cytoskeleton; nucleus
PDZ and LIM domain 1	**509**	DOWN	DOWN	Structural constituent of cytoskeleton; transcription factor activity; actin binding	Muscle contraction; regulation of transcription from RNA polymerase II promoter; cell motion; mesoderm development; cellular component morphogenesis; heart development; muscle organ development	Cytoplasm; cytoskeleton
Lipoma-preferred partner	**82**		DOWN	Structural constituent of cytoskeleton; protein binding; kinase regulator activity	Mitosis; cell motion; mitosis; signal transduction; mesoderm development; cellular component morphogenesis; muscle organ development	Nucleus; cytoplasm; cell membrane
LIM and SH3 domain protein 1	**102**		DOWN	Structural constituent of cytoskeleton; actin binding	Muscle contraction	Cytoplasm; cytoskeleton
Ezrin	**264**		DOWN	Structural constituent of cytoskeleton	Cellular component morphogenesis	Cell projection; cytoskeleton
Proteasome subunit alpha type-5	**185**	DOWN	UP	Peptidase activity	Proteolysis	Cytoplasm; nucleus
14-3-3 protein theta	**2**	DOWN	UP	Signal transduction	Cell cycle; signal transduction	Cytoplasm
60S acidic ribosomal protein P0	**338**	DOWN	UP	Structural constituent of ribosome; nucleic acid binding	Translation	Cytoplasm; nucleus
Aspartyl aminopeptidase	**132**	UP		Proteolysis	Aminopeptidase activity; metallopeptidase activity; zinc ion binding	Cytoplasm
Fascin	**125**	UP		Structural constituent of cytoskeleton; actin binding	Cell motion	Cytoskeleton; cell projection
Lamin A/C	**79**	UP		Structural constituent of cytoskeleton	Cellular component morphogenesis	Nucleus
GANAB protein	**330**	UP		Glucosidase activity	Polysaccharide metabolic process; monosaccharide metabolic process; protein modification process	Endoplasmic reticulum; golgi apparatus
Tubulin-specific chaperone E	**458**	UP		Post chaperonin tubulin folding pathway; protein folding; protein metabolic processes	Cellular component morphogenesis	Cytoskeleton
Serine hydroxymethyltransferase	**419**	UP		Methyltransferase activity	Nucleobase, nucleoside, nucleotide and nucleic acid metabolic process; cellular amino acid metabolic process	Mitochondrion
Annexin A11	**227**	UP		Calcium ion binding; calcium-dependent phospholipid binding	Synaptic vesicle exocytosis; intracellular protein transport;calcium-mediated signaling; fatty acid metabolic process; cell motion	Cytoplasm; nucleus
Moesin	**318**	UP	UP	Structural constituent of cytoskeleton	Cellular component morphogenesis	Cell membrane; cytoplasm; cell projection
Eukaryotic translation initiation factor 2 subunit 1	**573**	UP	UP	Translation factor activity, nucleic acid binding; translation initiation factor activity	Translation	Cytoplasm; nucleus
L-caldesmon	**110**	UP	UP	Structural constituent of cytoskeleton; actin binding	Mitosis; cellular component morphogenesis	Cytoskeleton
Osteoclast-stimulating factor 1	**40**	UP	UP	Signal transduction	SH3 domain binding	Cytoplasm
T-complex protein 1 subunit theta	**138;133**	UP	UP	Protein folding	Protein folding; protein complex assembly	Cytoplasm; cytoskeleton
BPI3V Phosphoprotein P	**27;182;92;44;47; 401;819;255;235**	UP	UP	Viral genome replication; transcription DNA - dependent	RNA-binding; RNA-directed RNA polymerase activity	NA
Protein disulfide-isomerase A3	**333;25**	UP	UP	Protein disulfide isomerase activity	Protein modification process	Endoplasmic Reticulum
Annexin	**16**		UP	Calcium ion binding; calcium-dependent phospholipid binding	Synaptic vesicle exocytosis; intracellular protein transport;exocytosis; calcium-mediated signaling; fatty acid metabolic process; cell motion	Cytoplasm; nucleus
Non-muscle myosin heavy chain	**48**		UP	Motor activity;structural constituent of cytoskeleton;protein binding;small GTPase regulator activity	Muscle contraction; sensory perception; intracellular protein transport; vesicle-mediated transport; cytokinesis; cell motion; mitosis; intracellular signaling cascade; cellular component morphogenesis; mesoderm development; muscle organ development	Cytoplasm; cell membrane
Nucleophosmin	**57**		UP	Intacellular protein transport; nucleasome and ribosome assembly; viral reproduction	rRNA metabolic process	Nucleus; cytoskeleton
6-phosphogluconolactonase	**62**		UP	Hydrolase activity	Pentose-phosphate shunt	Cytoplasm
14-3-3 protein beta/alpha	**111**		UP	Protein binding; innate immune response; apoptotic process; activation of MAPKK activity	Cell cycle; signal transduction; protein binding	Cytoplasm
Cystathionine gamma-lyase	**134**		UP	Lyase activity	Cellular amino acid metabolic process	Cytoplasm
Phosphoserine phosphatase	**158**		UP	Phosphatase activity	Cellular amino acid biosynthetic process	Cytoplasm
Heat shock 70 kDa protein	**5;166**		UP	Immune system process; protein folding; protein complex assembly; response to stress; protein complex biogenesis	Hsp70 family chaperone	Cytoplasm
Proteasome subunit beta type	**272**		UP	Proteolysis	Peptidase activity	Cytoplasm
Calponin-3	**357**		UP	Muscle contraction	Structural constituent of cytoekeleton; actin binding	Cytoskeleton
Isocitrate dehydrogenase [NAD] subunit alpha	**481**		UP	Generation of precursor metabolites and energy; carbohydrate metabolic process; tricarboxylic acid cycle	Oxidoreductase activity	Mitochondria
Eukaryotic translation initiation factor 6	**532**		UP	Translation; regulation of translation	Translation initiation factor activity	Cytoplasm